IOP Publishing | Astro Ltd Laser Physics

Laser Phys. **30** (2020) 095205 (10pp) https://doi.org/10.1088/1555-6611/aba7c4

Increasing efficiency of quantum memory based on atomic frequency combs

R N Shakhmuratov

Zavoisky Physical-Technical Institute, FRC Kazan Scientific Center of RAS, Kazan 420029, Russia

E-mail: shakhmuratov@mail.ru

Received 27 June 2020
Accepted for publication 14 July 2020
Published 21 August 2020

Abstract

A protocol, which essentially increases the efficiency of the quantum memory based on the atomic frequency comb (AFC), is proposed. It is well known that a weak short pulse, transmitted trough a medium with a periodic structure of absorption peaks separated by transparency windows (AFC), is transformed into prompt and delayed pulses. Time delay is equal to the inverse value of the frequency period of the peaks. It is proposed to send the prompt pulse again through the medium and to make both delayed pulses to interfere. This leads to the essential increase of the efficiency of the AFC storage protocol close to 100%.

Keywords: quantum memory, atomic frequency combs, optical transients

(Some figures may appear in colour only in the online journal)

1. Introduction

Single photons are ideal information carriers propagating fast a long distance with low losses. Controlling single photons is an important point in quantum computing and quantum telecommunication. One of the experimental challenges in quantum information science is a coherent and reversible light-matter mapping of quantum information carried by a single-photon wave packet. A light-state storage in collective atomic excitations for a pre-determined time is one of the ways to realize quantum memory crucial for quantum repeaters in quantum networks.

There are many schemes of quantum memory employing photon-echo technique [1, 2], controlled reversible inhomogeneous broadening (CRIB) protocol [3–5], electromagnetically induced transparency [6, 7], off-resonant Raman interaction [8–10]. The list of methods and related references are far to be exhausted. These methods suffer from contamination of the signal channel by spontaneous emission caused by the strong classical fields exciting auxiliary transitions in atoms or as in the case of CRIB protocol can be realized if optical transitions are sensitive to the electric fields controlling inhomogeneous broadening.

Passive schemes as, for example, atomic frequency comb (AFC) protocol [11–15], are preferable since passive protocols are capable to store quantum information in collective atomic excitations for a pre-determined time without using additional excitations complicating the storage schemes. Meanwhile, quantum efficiency of the AFC protocol, which is the first example of the passive scheme, is limited to 54% [12]. A lambda type excitation of AFC on an auxiliary transition by strong control fields is capable to increase quantum efficiency of the AFC protocol close to 100%, see reference [12]. However, combination of the passive AFC scheme with the auxiliary excitation also contaminates the quantum channel.

In this paper, a modification of the AFC protocol, which helps to improve the quantum efficiency without using additional fields, is proposed. A short pulse propagating through a medium with the AFC absorption spectrum is transformed into a prompt and delayed pulses at the exit of the medium. For the optimal values of the optical thickness of the medium and finesse of the comb the intensities (amplitudes) of the prompt and delayed pulses are $0.13I_0$ ($0.37E_0$) and $0.54I_0$ ($0.73E_0$), respectively, where I_0 and E_0 are maximum intensity and amplitude of the incident pulse. If the prompt pulse is transmitted again through the same AFC medium a new pulse

with the same delay time is produced. The amplitude of this pulse is $0.27E_0$. If we make two delayed pulses interfere constructively, the intensity of the produced pulse will be close to I_0. Physical constrains and limitations are considered in this paper.

2. Efficiency of the direct AFC protocol

In this section, the efficiency of the AFC quantum memory and results, obtained in references [11–15] are analyzed.

Frequency combs consisting of the absorption peaks separated by the transparency windows can be prepared in an inhomogeneously broadened absorption line of rare-iron doped crystals by different methods. One of them employs a long sequence of pulse pairs separated by time T, see references [11–14]. Each pair creates a frequency comb with a period $2\nu_0 = 2\pi/T$ due to pumping ground state atoms to a long-lived shelving state. Accumulative effect of many pairs of relatively weak pulses is capable to create deep holes in the inhomogeneously broadened absorption spectrum. Such a pumping creates a harmonic structure of an atomic population difference in the spectrum,

$$n(\Delta) = \frac{1}{2}\left[1 - \cos\left(\frac{\pi\Delta}{\nu_0}\right)\right], \tag{1}$$

where $\Delta = \omega_c - \omega_A$ is a frequency difference of a pulse carrier, ω_c, and individual atom in the comb, ω_A, see references [16, 17]. Here, atoms producing the absorption peaks occupy at their centers the ground state, while at the bottom of the transparency windows all atoms are removed to the shelving state. Inhomogeneous broadening is assumed to be very large. Therefore, the difference between the absorption peaks is neglected on the frequency scale comparable with a spectrum of optical pulses, which are filtered by the AFC.

In the other method, one creates a broad transmission hole by spectral hole burning and then periodic narrow-spectrum ensembles of atoms are created in the hole by repumping atoms from the storage state to the ground state [18–20]. Periodic structure of Loretzians, created by this method, was considered in references [13–15]. This structure is described by

$$n(\Delta) = \sum_{k=-N-1}^{N} \frac{\Gamma^2}{[\Delta + \nu_0(2k+1)]^2 + \Gamma^2}, \tag{2}$$

where $2\nu_0$ is the period of the comb, Γ is a halfwidth of the absorption peaks, and $2N+2$ is a number of peaks. It is also possible to create AFC with square-shaped absorption peaks of width 2δ separated by transparency windows. The distance between the centers of the absorption peaks is equal to $2\nu_0$. Then, the distribution of the atomic population difference in the inhomogeneously broadened absorption spectrum is described by the function

$$n(\Delta) = \sum_{n=-N-1}^{N} \{\theta[\Delta - (2k+1)\nu_0 + \delta] - \theta[\Delta - (2k+1)\nu_0 - \delta]\}, \tag{3}$$

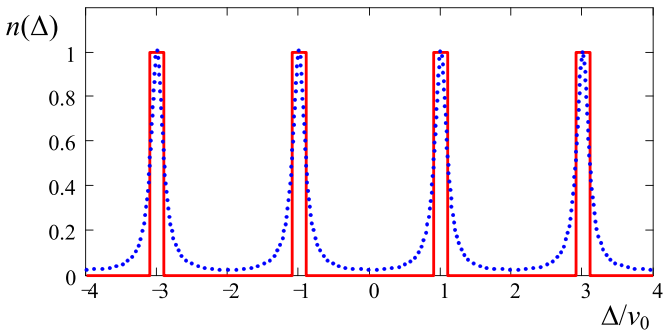

Figure 1. Frequency distribution of the population difference of atoms in the spectrum for AFC with square-shaped peaks (red solid line) and Lorentzian peaks (blue dotted line). The distance between the peak centers is $2\nu_0$. Half width of the peaks is δ for the square-shaped peaks and Γ for the Lorentzian peaks. They are $\delta = \Gamma = \nu_0/10$.

where $\theta(x)$ is the Heaviside step function. AFC with square-shaped absorption peaks are prepared in reference [13] by a differen method, which employs a pulse train with special relations of phases and amplitudes distributed according to the sinc function. Also, chirped light pulses with hyperbolic-secant complex amplitudes were used to built square-shaped absorption peaks in reference [15]. Examples of two AFCs with Lorentzian and square-shaped peaks are shown in figure 1. It is instructive to compare these two AFCs since they have tunable finesse, which is $F_S = \nu_0/\delta$ for the square-shaped AFC and $F_L = \nu_0/\Gamma$ for the Lorentzians. Finesse of the harmonic AFC, described by equation (1), is fixed and equal to $F_H = 2$. Therefore, this AFC can be compared with the other two when $F_S = F_L = 2$.

At the exit of the medium with a periodic absorption spectrum, a pulse with a spectrum covering many (or at least several) absorption peaks of the comb is transformed into a prompt pulse and several delayed pulses with delay times equal to T, $2T$, $3T$, etc, see references [11–17]. All the pulses have the same shape coinciding with the shape of the incident pulse. For the combs with high finesse, $F \gg 2$, and moderate optical thickness of the absorption peaks, only the prompt and first delayed pulses have noticeable amplitudes, see appendix A. Below we focus on the properties of these two pulses, which are

$$E_{out}(t) = E_p(t) + E_d(t-T), \tag{4}$$

where $E_{out}(t)$ is the field at the exit of the AFC medium, $E_p(t)$ is the prompt pulse with no delay, and $E_d(t-T)$ is the first delayed pulse, the amplitude of which takes maximum value at time $t = T$, while maximum of the prompt pulse is localized at $t = 0$ by definition.

Maximum amplitude of the prompt pulse $E_p(0) = C_0E_0$, where E_0 is a maximum amplitude of the incident pulse, is reduced by the coefficient C_0, which is

$$C_0 = \begin{cases} e^{-\frac{d_p}{2F_H}} & \text{harmonic} \\ e^{-\frac{\pi d_p}{4F_L}} & \text{Lorentzians,} \\ e^{-\frac{d_p}{2F_S}} & \text{squares} \end{cases} \tag{5}$$

see references [13–15, 17] and Appendix A. Here the label denotes the type of AFC, $d_p = \alpha l$ is an optical thickness of the medium for a monochromatic field tuned in resonance with one of the absorption peaks, α is the corresponding Beer's law attenuation coefficient, l is a physical thickness of the medium, and F is finesse of the comb, which is $F_H = 2$, $F_L = \nu_0/\Gamma$ or $F_S = \nu_0/\delta$ depending on the selected AFC.

Maximum amplitude of the first delayed pulse is $E_d(0) = C_1 E_0$, where

$$C_1 = C_0 \times \begin{cases} \frac{d_p}{2F_H} & \text{harmonic} \\ \frac{\pi d_p}{2F_L} e^{-\frac{\pi}{F_L}} & \text{Lorentzians} \\ \frac{d_p}{\pi} \sin\left(\frac{\pi}{F_S}\right) & \text{squares,} \end{cases} \tag{6}$$

C_0 is the coefficient in equation (5), corresponding to the relevant comb, see references [13–15, 17] and Appendix A. The coefficient C_1 takes global maximum value when $C_0 = e^{-1}$. This value is achieved if the optical depth d_p is equal to 4 for the harmonic comb, $4F_L/\pi$ for the comb of Lorentzian peaks, and $2F_S$ for the square comb. For these values of d_p and large finesse satisfying the condition $F_{L,S} \gg \pi$, we have

$$C_1 = e^{-1} \times \begin{cases} 1 & \text{harmonic} \\ 2e^{-\frac{\pi}{F_L}} & \text{Lorentzians} \\ 2 & \text{squares.} \end{cases} \tag{7}$$

Extra exponent for the comb of Lorentzians originates from the inhomogeneous broadening of the absorption peaks with Lorentzian wings, which give $\exp(-\pi/F_L) = \exp(-\Gamma T)$. Therefore, the square-shaped comb produces the first delayed pulse with larger amplitude for moderate values of finesse ($F_S > \pi$) compared with the comb consisting of the Lorentzian peaks.

Meanwhile, an abrupt drop of the wings of the square-shaped peaks results in the function $\sim \sin\left(\frac{\pi}{F_S}\right)$, see equation (6), which also reduces the amplitude of the first delayed pulse produced by the pulse filtering through this comb with a moderate value of finesse.

The intensity of the first delayed pulse is defined by the equation $I_1 = C_1^2 I_0$, where I_0 is a maximum intensity of the incident pulse. Dependence of the coefficient

$$C_1^2 = \left(\frac{d_p}{\pi}\right)^2 \sin^2\left(\frac{\pi}{F_S}\right) e^{-\frac{d_p}{F_S}} \tag{8}$$

for the square comb on d_p for different values of the finesse F_S is shown in figure 2(a). For example, for $F_S = 2$ the optimal value of the optical thickness is $d_p = 4$ and corresponding global maximum of the first delayed pulse is $I_1 = 0.219 I_0$. For the harmonic frequency comb, this global maximum is even smaller and equals to $I_1 = e^{-2} I_0 = 0.135 I_0$. With the increase of F_S or with narrowing of the absorption peaks at the fixed width of the transparency windows, the optimal value of d_p also increases according to the relation $d_p = 2F_S$ and the optimal intensity of the first delayed pulse, I_1, corresponding to the global maximum rises, see Figure 2(b). For

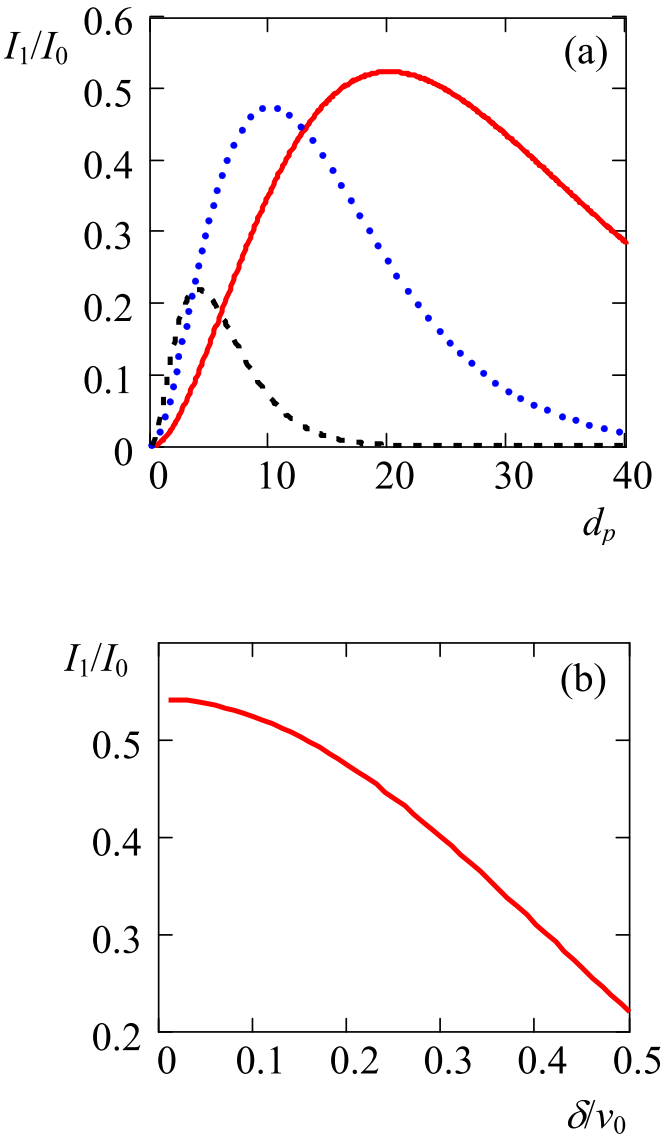

Figure 2. (a) Dependence of the maximum intensity of the first delayed pulse (normalized to I_0) on the peak absorption parameter d_p for the finesse $F = 10$ (solid red line), 5 (dotted blue line), and 2 (dashed black line). (b) Dependence of the intensity I_1/I_0 on the inverse value of the finesse $1/F_S = \delta/\nu_0$ if $d_p = 2F_S$, which is the condition when this intensity has a global maximum.

example, for $F_S = 10$ the optimal value of d_p is 20 and maximum value of I_1 is $0.524 I_0$. If large finesse F_S does not correspond to the optimal value of the optical thickness $d_p/2$, then maximum value of I_1 decreases. For example, for $d_p = 2$ and $F_S = 10$, the maximum amplitude of the first delayed pulse is $I_1 = 0.104 I_0$, which is almost five times smaller than that for the optimal values of the parameters $d_p = 20$ and $F_S = 10$.

Maximum efficiency of the AFC quantum memory, 54%, is achieved for a very large values of finesse and optical thickness. For the square-shaped comb this efficiency is realized when $F_S = 32$ and $d = 64$.

Actually, it is difficult to create AFC in an optically dense medium since the hole burning field is strongly absorbed along the sample of large optical thickness. Therefore, the hole width

becomes inhomogeneous along the sample, *i.e.* broader at the one side and narrower at the other side. However, this problem could be solved in a planar geometry where a medium is thick in a longitudinal direction and relatively thin in a transverse direction. Then, illuminating along a thin direction with low absorption creates a sequence of holes, while a weak signal pulse propagating in the longitudinal direction with high absorption at particular frequencies periodically distributed in a wide transparency window experiences the necessary splitting into prompt and delayed pulses. The sequence of holes can be produced by creating a large spectral hole and then transferring back atoms from an auxiliary state to create a comb as described in references [18–20]. If collinear pulses producing AFC illuminate the sample perpendicular to its thin side, no spatial grating is created and AFC will be spatially homogeneous along its thick direction.

Such a geometry was used in reference [21] to create narrowband spectral filter, which consists of a planar waveguide, covered with a thin polymer film containing molecules. They undergo spectral hole burning at liquid helium temperature creating transparency window at a selected frequency. Such a scheme of the hole burning was proposed in reference [22] to delay short pulses transmitting them trough an optically thick sample with a single transparent hole.

3. Limitations imposed by the homogeneous broadening of the absorption lines of individual atoms

In this section the influence of the homogeneous broadening of the absorption peaks of the comb on the pulse propagation is considered.

To take into account the contribution of the homogeneous broadening we consider the evolution of the nondiagonal element of the atomic density matrix $\rho_{eg}(z,t)$ describing coherence between ground g and excited e states of an atom. In the linear response approximation neglecting the change of the populations g and e, the slowly varying complex amplitude of the atomic coherence, $\sigma_{eg}(z,t)=\rho_{eg}(z,t)\exp(i\omega_c t-ik_c z)$, satisfies the equation

$$\frac{\partial}{\partial t}\sigma_{eg}(z,t)=(i\Delta-\gamma)\sigma_{eg}(z,t)+i\Omega(z,t)n(\Delta), \tag{9}$$

where γ is the decay rate of the atomic coherence responsible for the homogeneous broadening of the absorption line of a single atom, $\Delta=\omega_c-\omega_A$ is the difference of the frequency ω_c of the weak pulsed field and resonant frequency ω_A of an individual atom, $\Omega(t)=\mu_{eg}E_0(z,t)/2\hbar$ is the Rabi frequency, μ_{eg} is the dipole-transition matrix element between g and e states, and $n(\Delta)$ is the long-lived population difference, created by the hole burning. Below, we consider the square-shaped distribution of atoms in the frequency domain, shown in figure 1 by the solid red line. Then, the function $n(\Delta)$ is equal unity if atom is in the ground state absorbing the resonant field, and $n(\Delta)$ is zero if atom with the frequency $\omega_A=\omega_c-\Delta$ is removed by the hole burning to the shelving state resulting in the appearance of the transparency window.

The Fourier transformation of equation (9) gives the solution

$$\sigma_{eg}(z,\nu)=-\frac{\Omega(z,\nu)n(\Delta)}{\nu+\Delta+i\gamma}. \tag{10}$$

With the help of the Fourier transformation of the wave equation

$$\widehat{L}E_0(z,t)=i\hbar\alpha\gamma\left\langle\sigma_{eg}(z,t)\right\rangle/\mu_{eg}, \tag{11}$$

one can obtain the solution

$$E_0(z,\nu)=E_0(0,\nu)\exp[(i\nu z/c)-\alpha_{\rm av}(\nu)z/2], \tag{12}$$

where $L=\partial_z+c^{-1}\partial_t$, $\alpha=4\pi\omega_c N|\mu_{eg}|^2/\gamma\hbar c$ is the absorption coefficient before the hole burning, N is the density of atoms, $\langle\sigma_{eg}(z,t)\rangle$ is the atomic coherence integrated over inhomogeneous broadening with the width $\Gamma_{\rm inh}$, and

$$\alpha_{\rm av}(\nu)=i\frac{\alpha\gamma}{\pi\Gamma_{\rm inh}}\int_{-\infty}^{+\infty}\frac{n(\Delta)}{\nu+\Delta+i\gamma}d\Delta. \tag{13}$$

If inhomogeneous broadening is large enough that the absorption peaks of the AFC can be considered as having the same height over the frequency range covered by the spectrum of the incident pulse, then the complex coefficient $\alpha_{\rm av}(\nu)$ is reduced to

$$\alpha_{\rm av}(\nu)=\alpha[\epsilon''(\nu)-i\epsilon'(\nu)], \tag{14}$$

where

$$\epsilon''(\nu)=\frac{1}{\pi}\sum_{k=-N-1}^{N}\left\{\tan^{-1}\left[\frac{\nu+\delta+(2k+1)\nu_0}{\gamma}\right]-\tan^{-1}\left[\frac{\nu-\delta+(2k+1)\nu_0}{\gamma}\right]\right\}, \tag{15}$$

$$\epsilon'(\nu)=-\frac{1}{2\pi}\sum_{k=-N-1}^{N}\ln\left[\frac{[\nu+\delta+(2k+1)\nu_0]^2+\gamma^2}{[\nu-\delta+(2k+1)\nu_0]^2+\gamma^2}\right]. \tag{16}$$

Here, $2N+2$ is the number of the absorption peaks in the comb. The plots of the functions $\epsilon''(\nu)$ and $\epsilon'(\nu)$ are shown in figure 3. It is seen that the edges of the absorption peaks are smoothened due to the contribution of the Lorentzian in equation (13) originating from the response of atoms with population difference $n(\Delta)$ neighboring the frequency component ν. The wings of the Lorentzians also contribute to the absorption at the centers of the transparency windows where, for example, at $\nu=0$ we have

$$\epsilon''(0)\approx\frac{4}{\pi}\sum_{k=0}^{N}\frac{\gamma\delta}{(2k+1)^2\nu_0^2-\delta^2}. \tag{17}$$

If finesse F is 10, and $\gamma/\delta=0.1$, then due to the contribution of the Lorentzians, the absorption at the center of the transparency window rises from zero to 1.54×10^{-4}. For the optimal value of the thickness d_p, which is 20 for $F_S=10$,

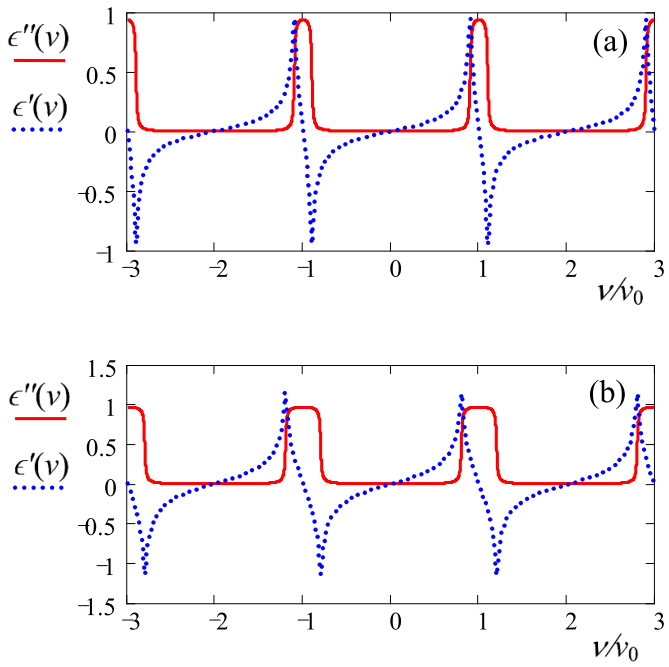

Figure 3. (a) Absorption, $\epsilon''(\nu)$, (red solid line) and dispersion, $\epsilon'(\nu)$, (blue dotted line) of the AFC, convoluted with Lorentzians, see equations (13)–(16). Parameters of the comb are $\delta/\nu_0 = 0.1$ (a) and 0.2 (b). Decay rate of the atomic coherence is the same in both plots, which is $\gamma = 0.01\nu_0$.

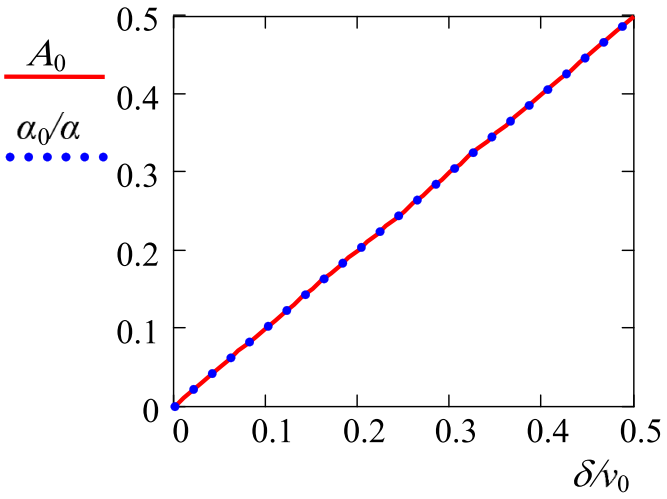

Figure 4. Dependencies of the coefficient α_0/α (dotted blue line) and numerically calculated coefficient A_0 (red solid line) on δ/ν_0 for a fixed value of ν_0. Homogeneous decay rate of the coherence is $\gamma = 0.01\nu_0$.

the intensity of a monochromatic radiation field tuned at the center of the transparency window is reduced by a factor of $\exp[-d_p\epsilon''(0)] = 0.97$, *i.e.* it drops by 3%. Moreover, maximum of the absorption peaks decreases due to the homogeneous broadening. For example, the coefficient $\epsilon''(\nu)$ at $\nu = \nu_0$ decreases as

$$\epsilon''(\nu_0) \approx 1 - \frac{2}{\pi}\left(\frac{\gamma}{\delta} - \frac{2\gamma\delta}{4\nu_0^2 - \delta^2}\right). \tag{18}$$

The drop of absorption is noticeable. For the same example, considered for the transparency windows ($F_S = 10$ and $\gamma/\delta = 0.1$), we have $\epsilon''(\nu_0) = 0.937$, *i.e.* the absorption coefficient drops by 6.3% at the centers of the absorption peaks. To reduce this drop one has to decrease the ratio γ/δ increasing the values of δ and ν_0.

From the solution, equation (12), one finds that the prompt pulse and the first delayed pulse are described by equation

$$E_{\text{out}}(t) = e^{-A_0 d_p/2}\left[E_{\text{in}}(t) + A_1\frac{d_p}{2}E_{\text{in}}(t-T)\right], \tag{19}$$

where small term $i\nu l/c$ is neglected, and

$$A_0 = \frac{1}{2\nu_0}\int_{-\nu_0}^{\nu_0}\epsilon''(\nu)d\nu, \tag{20}$$

$$A_1 = -\frac{1}{2\nu_0}\int_{-\nu_0}^{\nu_0}[\epsilon''(\nu) - i\epsilon'(\nu)]\,e^{-i\pi\nu/\nu_0}d\nu. \tag{21}$$

From the Kramers-Kronig relations, it follows that the coefficient A_1 is reduced to

$$A_1 = -\frac{1}{\nu_0}\int_{-\nu_0}^{\nu_0}\epsilon''(\nu)e^{-i\pi\nu/\nu_0}d\nu. \tag{22}$$

In spite of the difference between the complex coefficient $\alpha_{\text{av}}(\nu) = \alpha[\epsilon''(\nu) - i\epsilon'(\nu)]$, averaged with Lorentzian, equation (13), and the complex coefficient $\alpha_c(\nu) = \alpha[\chi''(\nu) - i\chi'(\nu)]/\chi_M$, which is not averaged, see equation (A10) in the appendix A, the coefficients reducing the absorption of the prompt pulse, which are proportional to A_0, equation (20), for the first function and α_0/α, equation (A13), for the second function, are the same, *i.e.* $\alpha_0/\alpha = A_0 = \delta/\nu_0$. These coefficients equal to the inverse value of the finesse $F_S^{-1} = \delta/\nu_0$, which is the same for both combs. This is almost obvious result. However, as it was mentioned above, the heights of the absorption peaks and the depths of the transmission windows of these combs are different and one could expect that the values of the integrals A_0 in equation (20) and α_0/α in equation (A13) responsible for the decrease of the amplitude of the prompt pulse are also different. Dependencies of $\alpha_0/\alpha = \delta/\nu_0$ and numerically calculated A_0 on δ for the fixed values of ν_0 and γ are compared in figure 4 demonstrating that the above conclusion about the same relation of the coefficients with the finesse, based on the analytical calculation, is correct. Moreover, the dependence $A_0 = \delta/\nu_0$ is still valid if $\gamma = 0.1\nu_0$, *i.e.* when the coherence decay rate γ is an order of magnitude larger than in the previous example.

The coefficients A_1 and $-\alpha_1/\alpha \sim a_1$ in the solutions equation (19) and equation (A15), respectively, which define the amplitude of the first delayed pulse, are also very close to each other, *i.e.* $-\alpha_1/\alpha = 2\sin\left(\frac{\pi\delta}{\nu_0}\right)/\pi$ and

$$A_1 = 2\frac{\sin\left(\frac{\pi\delta}{\nu_0}\right)}{\pi}e^{-\frac{\pi\gamma}{\nu_0}}. \tag{23}$$

The exponential factor $\exp(-\pi\gamma/\nu_0) = \exp(-T/T_2)$, where $T_2 = 1/\gamma$, is the homogeneous dephasing time, has little influence on the amplitude of the first delayed pulse if $T \ll T_2$. It can be shown, see reference [17], that exactly the same factor, $\exp(-T/T_2)$, appears due to the homogeneous dephasing in the expression for the amplitude of the first delayed pulse C_1E_0, see equation (6), for the AFSs consisting of harmonic and Lorentzian peaks.

Experimental verifications of the AFC storage protocol were performed in Nd^{3+} ions, doped into YVO_4, reference [11], and YAG (Tm^{3+} : YAG)), [13–15]. Relatively large efficiency (9–18 %) in references [13–15] was achieved for the moderate value of the initial absorption (before pumping) described by the parameter $d_p \sim 4-5$. After the hole burning this parameter reduced to $d_p \sim 3$, see references [13–15]. The best performance of this memory is achieved for the square-shaped AFC [13, 15] with different values of finesse $F_S = 2$, 3, and 5.

If we take the following values of the AFC parameters realized in reference [15], *i.e.* $2\nu_0 = 2$ MHz, $2\delta = 400$ kHz, and $\gamma = 5$ kHz, then the maximum intensity of the first delayed pulse,

$$I_1 = \left(\frac{d_p}{\pi}\right)^2 \sin^2\left(\frac{\pi}{F_S}\right) e^{-\frac{d_p}{F_S} - 2\gamma T} I_0, \tag{24}$$

is nearly 17% of the incident pulse. Finesse of such a comb is $F_S = 5$. Actually, the optimal thickness of the sample should be $d_p = 2F_S = 10$, which is only three times larger than that ($d_p \sim 3$), realized in the experiments [13–15]. For $d_p = 10$, which is optimal in this case, the efficiency increases to 46%.

4. Second treatment of the prompt and delayed pulses

If we split the optical paths of the prompt and first delayed pulses by time-division multiplexing and send the prompt pulse again through the AFC medium with the same parameters or backward through the same AFC, we transform the prompt pulse into new pair of pulses, *i.e.* the prompt and delayed. This pair is described by the equation

$$E_{\text{out}}(t) = e^{-A_0 d_p}\left[E_{\text{in}}(t) + A_1 \frac{d_p}{2} E_{\text{in}}(t-T)\right], \tag{25}$$

where exponential factor $e^{-A_0 d_p}$ differs from that, $e^{-A_0 d_p/2}$, in equation (19) due to absorption in the second path through the AFC medium. Then, one can make the paths of two delayed pulses such that both pulses arrive to the selected point at the same time and with the same phase and then travel together. Their sum is described by the equation

$$E_{\text{d}}(t-T) = A_1 \frac{d_p}{2}\left(e^{-A_0 d_p/2} + e^{-A_0 d_p}\right) E_{\text{in}}(t-T), \tag{26}$$

where small delay time of the pulses due to traveling trough the optical paths of some length L with a speed of light c is disregarded. Due to constructive interference of the fields the intensity of this sum field is

$$I_{\text{d}}(t-T) = \left(\frac{A_1 d_p}{2}\right)^2 e^{-A_0 d_p}\left(1 + e^{-A_0 d_p/2}\right)^2 I_0. \tag{27}$$

If we take the following optimal values of the parameters for the square-shaped AFC, considered at the end of section 3, *i.e.* $F_S = 5$, $2\nu_0 = 2$ MHz, $\gamma = 5$ kHz , and $d_p = 2F_S = 10$, then the intensity of the field $I_d(0)$ increases to 86% of the intensity of the incident pulse. The medium with $d_p = 2F_S = 20$ gives even better efficiency, which is 95%. Further increase of the efficiency of the AFC quantum memory is possible by increasing the frequency spacing of the comb, $2\nu_0$, with respect to the homogeneous width γ, or by choosing a medium with smaller value of γ.

This protocol of quantum storage can be applied to store time-bin qubits, which in the simplest case can be described as

$$|\Psi\rangle = C_1|\Psi_1\rangle + e^{i\varphi} C_2|\Psi_2\rangle. \tag{28}$$

Here $|\Psi\rangle$ is a single photon state, which is a superposition of states $|\Psi_1\rangle$ and $|\Psi_2\rangle$ corresponding to two short pulses separated in time and forming time bins, see references [23, 24]. Quantum information is encoded in the probability amplitudes C_1, C_2 and their relative phase φ. These states can be prepared with an unbalance Mach-Zehnder interferometer, see references [23, 24] for details. Partial readouts of the states can be implemented by the same unbalanced Mach-Zehnder interferometer. Meanwhile, these readouts can be performed using a double-AFC structure with the frequency periods $2\nu_1$ and $2\nu_2$, see references [11, 25]. If the time, τ, between pulses in the time-bin qubit matches the time difference in delay $\pi(1/\nu_1 - 1/\nu_2)$, the re-emission from the AFC filters can be suppressed or enhanced depending on the phase φ. We do not consider these combined AFC filters in the storage stage.

We consider the case when time interval between pulses is $\tau < T$ and they have Gaussian envelopes $\propto e^{-\sigma^2(t\pm\tau/2)^2}$, with $+\tau$ for $|\Psi_1\rangle$ and $-\tau$ for $|\Psi_2\rangle$. The transformation of these states after passing through the square AFC is discussed in the appendix B. Experimental storage and retrieval of multiple photonic qubits (qudits) consisting of the train of many pulses is demonstrated in references [11, 25].

If the train consists of two pulses, after passing through the square AFC the state $|\Psi\rangle$ is transformed as

$$|\Psi\rangle_{\text{tr}} = C_{1p}|\Psi_1\rangle_p + e^{i\varphi} C_{2p}|\Psi_2\rangle_p + C_{1d}|\Psi_1\rangle_d + e^{i\varphi} C_{2d}|\Psi_2\rangle_d, \tag{29}$$

where $|\Psi_{1,2}\rangle_p$ is a couple of photon states with no delay (prompt pulses) and $|\Psi_{1,2}\rangle_d$ is a couple of states (actually wave packets) delayed by time T. The coefficients in equation (29) are $C_{1p} = C_1 e^{-A_0 d_p/2}$, $C_{2p} = C_2 e^{-A_0 d_p/2}$ and $C_{1d} = C_{1p} A_1 d_p/2$, $C_{2d} = C_{2p} A_1 d_p/2$. The phase factor $e^{i\varphi}$ and relation between the probability amplitudes of the states $|\Psi_{1,2}\rangle_d$ are the same as for the initial state $|\Psi\rangle$, equation (28). If delay time T is much longer than time separation τ between pulses in the qubit, the prompt pulses are well separated from the

delayed pulses. Sending the couple of prompt pulses again through the AFC and making constructive interference of the delayed pulses from both paths we obtain

$$|\Psi\rangle_{\rm int} = \mathcal{C}_{1p}|\Psi_1\rangle_p + e^{i\varphi}\mathcal{C}_{2p}|\Psi_2\rangle_p + \mathcal{C}_{1d}|\Psi_1\rangle_d + e^{i\varphi}\mathcal{C}_{2d}|\Psi_2\rangle_d, \tag{30}$$

where $\mathcal{C}_{1p} = C_1 e^{-A_0 d_p}$, $\mathcal{C}_{2p} = C_2 e^{-A_0 d_p}$ and $\mathcal{C}_{1d} = C_{1p}(1 + e^{-A_0 d_p/2})A_1 d_p/2$, $\mathcal{C}_{2d} = C_{2p}(1 + e^{-A_0 d_p/2})A_1 d_p/2$. The probabilities of the delayed pulses are described by equations

$$|\mathcal{C}_{1d}|^2 = \left(\frac{A_1 d_p}{2}\right)^2 e^{-A_0 d_p}\left(1 + e^{-A_0 d_p/2}\right)^2 |C_1|^2, \tag{31}$$

$$|\mathcal{C}_{2d}|^2 = \left(\frac{A_1 d_p}{2}\right)^2 e^{-A_0 d_p}\left(1 + e^{-A_0 d_p/2}\right)^2 |C_2|^2. \tag{32}$$

Their forms are exactly the same as for the intensity of the classical field in equation (27). Therefore, the conclusion made about efficiency increasing of the modified AFC memory is also valid for the time-bin quantum states.

5. Conclusion

The propagation of the light pulse in a medium with the periodic structure in the absorption spectrum is analyzed. It is shown that AFCs with the square-shaped absorption peaks in the spectrum demonstrate larger efficiency of the field storage. The influence of the homogeneous decay of the atomic coherence on the quantum efficiency is considered. It is proposed to send the prompt pulse, transmitted through the AFC medium, to the same medium again and to make interfere two delayed pulses, *i.e.* the delayed pulse transmitted trough the first AFC with the delayed pulse transmitted trough the second AFC. It is shown that for the optimal parameters of the AFC filters, one can increase the intensity of the delayed pulse close to the intensity of the pulse to be stored.

It should be noted that generally AFC quantum memory can be constructed out of small size crystals or any other absorbing medium with narrow resonances. For example, AFC experiments with thulium-doped YAG (Tm^{3+}:YAG)) [15] were performed in 5 mm length crystal. Short pulses were delayed in this small crystal by 500 ns. The same delay of the pulse in open air needs distance 150 m, while in optical fiber - 100 m, respectively. Thus, AFC quantum memory allows to shorten the size of such a delay line at least $\sim 10^4$ times.

Atomic ensembles with a comb spectrum can be replaced by micro-cavities, see, for example [26, 27] and references therein. Recently, it was designed multiresonant high-Q plasmonic metasurfaces generating narrow optical resonances enabling applications in filtering akin to AFC [28]. Similar proposal for high-Q multiband near-infrared wave absorption based on Si-Au nanowire resonator is repotrted in [29]. Therefore, one can expect wide applications of the AFC method in materials and devices, which work as comb-like filters of optical pulses.

Acknowledgment

This work was funded by the government assignment from the Federal Research Center 'Kazan Scientific Center of the Russian Academy of Sciences.'

Appendix A.

In this appendix the propagation of a short pulse through a medium with the square AFC in its spectrum is considered. The wave equation, describing the propagation of the pulsed field $E(z,t) = E_0(z,t)\exp(-i\omega_c t + ikz)$ along axis **z**, is (see, for example, reference [30])

$$\left(\frac{\partial}{\partial z} + \frac{n}{c}\frac{\partial}{\partial t}\right)E_0(z,t) = i\frac{2\pi\omega_c}{nc}P_0(z,t), \tag{A1}$$

where $E_0(z,t)$ is the pulse envelope, k is the wave number, n is the index of refraction, and $P(z,t) = P_0(z,t)\exp(-i\omega_c t + ikz)$ is the polarization induced in the medium.

The Fourier transform,

$$F(\nu) = \int_{-\infty}^{+\infty} f(t)e^{i\nu t}dt, \tag{A2}$$

of the field and polarization satisfy the relation $P(z,\nu) = \varepsilon_0\chi(\nu)E_0(z,\nu)$, where $\nu = \omega_c - \omega$ is the frequency difference between the central frequency of the light pulse ω_c and its spectral component ω, ε_0 is the electric permittivity of free space (below we set $\varepsilon_0 = 1$ and $n = 1$ for simplicity) and $\chi(\nu)$ is the electric susceptibility, which is

$$\chi(\nu) = \chi'(\nu) + i\chi''(\nu). \tag{A3}$$

By the Fourier transform the wave equation, equation (A1), is reduced to a one-dimensional differential equation, the solution of which is (see reference [30])

$$E_0(z,\nu) = E_0(0,\nu)\exp\left\{i\nu\frac{z}{c} - \frac{\alpha z}{2\chi_M}\left[\chi''(\nu) - i\chi'(\nu)\right]\right\}, \tag{A4}$$

where $E_0(0,\nu) = E_{in}(\nu)$ is a spectral component of the field incident to the medium, α is the Beer's law attenuation coefficient describing absorption of a monochromatic field tuned in maximum of the absorption line where $\chi''(0) = \chi_M$ and $\chi'(0) = 0$. One can introduce a frequency dependent complex coefficient

$$\alpha_c(\nu) = \alpha\frac{\chi''(\nu) - i\chi'(\nu)}{\chi_M}, \tag{A5}$$

which takes into account the contributions of absorption and dispersion.

The imaginary part of susceptibility, $\chi''(\nu)$, describes the field absorption. We consider AFC with the square-shaped absorption peaks of width 2δ separated by transparency windows. The distance between the centers of the absorption peaks is equal to $2\nu_0$. To make simple analytical treatment we take Fourier transform of this periodic structure and limit our

consideration to the $2N+1$ spectral components. Then, $\chi''(\nu)$ is expressed as follows

$$\chi''(\nu)/\chi_M = \frac{\delta}{\nu_0} + \frac{2}{\pi}\sum_{k=1}^{N}(-1)^k \frac{\sin\left(\frac{k\pi\delta}{\nu_0}\right)\cos\left(\frac{k\pi\nu}{\nu_0}\right)}{k}. \quad \text{(A6)}$$

Here k is an integer and inhomogeneous width of the absorption line, where the frequency comb is prepared, is approximated as infinite. The central frequency of the comb, $\nu = 0$, coincides with the center of one of the transparency windows corresponding to no absorption in the ideal case. The height of the absorption peaks corresponds to the absorption of the medium before the comb preparation.

The real part of the susceptibility, responsible for a group velocity dispersion, satisfies one of the Kramers-Kronig relations

$$\chi'(\nu) = \frac{1}{\pi}\mathcal{P}\int_{-\infty}^{\infty}\frac{\chi''(\nu')}{\nu'-\nu}d\nu', \quad \text{(A7)}$$

where $\mathcal{P}$ denotes the Cauchy principal value. Calculating the integral, we obtain

$$\chi'(\nu)/\chi_M = -\frac{2}{\pi}\sum_{k=1}^{N}(-1)^k \frac{\sin\left(\frac{k\pi\delta}{\nu_0}\right)\sin\left(\frac{k\pi\nu}{\nu_0}\right)}{k}. \quad \text{(A8)}$$

Frequency dependencies of the absorption $\sim\chi''(\nu)$ and dispersion $\sim\chi'(\nu)$ of the medium with the selected periodic spectrum are shown in figure A1.

Thus, the Fourier transform of the solution of the wave equation (A1),

$$E_0(z,\nu) = E_0(0,\nu)\exp\left[-\alpha_c(\nu)z/2\right], \quad \text{(A9)}$$

where small term $i\nu z/c$ is neglected, contains the complex coefficient

$$\alpha_c(\nu)/\alpha = \frac{\delta}{\nu_0} + \frac{2}{\pi}\sum_{k=1}^{N}(-1)^k \frac{\sin\left(\frac{k\pi\delta}{\nu_0}\right)}{k}e^{ik\pi\nu/\nu_0}, \quad \text{(A10)}$$

which takes into account absorption and dispersion. Their contributions to the harmonics $e^{ik\pi\nu/\nu_0}$ are equal, while the central part, δ/ν_0, originates only from the absorption.

Similar dependence of $\alpha_c(\nu)$ can be derived for any shape of the absorption peaks since in general for a periodic function $\alpha_c(\nu)$ we have

$$\alpha_c(\nu) = \sum_{k=0}^{\infty}\alpha_k e^{ik\pi\nu/\nu_0}, \quad \text{(A11)}$$

where

$$\alpha_k = \frac{1}{2\nu_0}\int_{-\nu_0}^{\nu_0}\alpha_c(\nu)e^{-ik\nu}d\nu. \quad \text{(A12)}$$

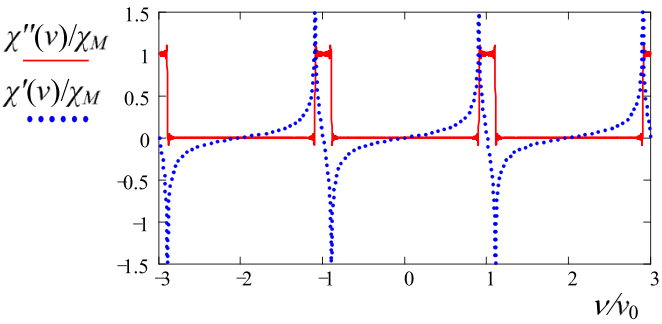

Figure A1. Absorption, $\chi''(\nu)$, (red solid line) and dispersion, $\chi'(\nu)$, (blue dotted line) components of the AFC with square-shaped absorption peaks of width $2\delta = \nu_0/5$ separated by the transparency windows. Both functions are normalized to $\chi_0(\nu)$. Frequency scale is in units of ν_0.

Equations (A10) and (A11) contain only positive k due to the Kramers-Kronig relations. These relations also allow essential simplification of the expression for α_k, which can be reduced to

$$\alpha_0 = \frac{\alpha}{2\nu_0}\int_{-\nu_0}^{\nu_0}\frac{\chi''(\nu)}{\chi_M}d\nu, \quad \text{(A13)}$$

and

$$\alpha_k = \frac{\alpha}{\nu_0}\int_{-\nu_0}^{\nu_0}\frac{\chi''(\nu)}{\chi_M}e^{-ik\nu}d\nu \quad \text{(A14)}$$

for $k>0$. In the coefficient α_0 the dispersion contribution is zero since it is odd function, while in α_k $(k>0)$ dispersion, $\chi'(\nu)$, contributes exactly the same value as the absorption, $\chi''(\nu)$. For the same reason the exponents $e^{ik\pi\nu/\nu_0}$ with negative k are absent in equation (A11) since for them the contributions of $\chi'(\nu)$ and $\chi''(\nu)$ are canceled.

With the help of the expansion of the function $\exp\left[-\alpha_c(\nu)z\right]$ in a power series of $\exp(i\pi\nu/\nu_0)$ one finds

$$E_0(l,\nu) = E_{in}(\nu)e^{-d_p/2F_S}\sum_{k=0}^{+\infty}a_k e^{i\pi k\nu/\nu_0}, \quad \text{(A15)}$$

where $d_p = \alpha_M l$, l is the physical length of the medium, $a_0 = 1$, $a_1 = \frac{d_p}{\pi}\sin(\pi/F_S)$,

$$a_2 = -\frac{d_p}{2\pi}\sin\left(\frac{2\pi}{F_S}\right) + \frac{d_p^2}{2\pi^2}\sin^2\left(\frac{\pi}{F_S}\right), \quad \text{(A16)}$$

$$a_3 = \frac{d_p}{3\pi}\sin\left(\frac{3\pi}{F_S}\right) - \frac{d_p^2}{2\pi^2}\sin\left(\frac{\pi}{F_S}\right)\sin\left(\frac{2\pi}{F_S}\right) + \frac{d_p^3}{6\pi^3}\sin^3\left(\frac{\pi}{F_S}\right), \quad \text{(A17)}$$

etc.

The inverse Fourier transformation of $E_0(l,\nu)$,

$$E_0(l,t) = \frac{1}{2\pi}\int_{-\infty}^{+\infty}E_0(l,\nu)e^{-i\nu t}dt, \quad \text{(A18)}$$

gives the solution

$$E_{\text{out}}(t) = e^{-d_p/2F_S} \sum_{k=0}^{+\infty} a_k E_{\text{in}}(t - kT), \qquad \text{(A19)}$$

where $E_{\text{out}}(t) = E_0(l,t)$ is the field at the exit of of the medium and $T = \pi/\nu_0$ is a delay time. Maximum amplitude of the prompt pulse with $k = 0$ in equation (A19) decreases according to the equation $E_{\text{pr}} = e^{-d_{\text{eff}}/2} E_0$ where effective thickness $d_{\text{eff}} = d_p/F_S$ is reduced with respect to d_p by a factor of finesse of the square comb, $F_S = \nu_0/\delta$. Maximum amplitude of the first delayed pulse with $k = 1$ is described by the equation $E_1 = a_1 e^{-d_{\text{eff}}/2} E_0$ where $a_1 = \frac{d_{\text{eff}} F_S}{\pi} \sin(\pi/F_S)$. Maximum intensity of this pulse $I_1 = |E_1|^2$ has a global maximum $I_{\text{gl}} = \left(\frac{2F_S}{\pi}\right)^2 \sin^2(\pi/F_S) e^{-2} I_0$ for $d_{\text{eff}} = 2$ or $d_p = 2F_S$ where $I_0 = |E_0|^2$. Dependence of I_{gl} on the inverse value of finesse, $1/F_S$, is shown in figure 2(b). From this figure, it follows that efficiency of the AFC memory, I_{gl}/I_0, increases with increasing finesse. The parameter d_p corresponding to this efficiency also increases according to the relation $d_p = 2F_S$.

It is interesting to notice that for a large finesse and the optimal value of optical thickness, $d_p = 2F_S$, of moderate value the incident field after passing through AFC medium is mainly distributed between the prompt and first delayed pulses, see figure A2(b). While, for the lowest finesse value $F = 2$, the amplitude of the pulse delayed by time 2 T (the second delayed pulse) is comparable with the amplitudes of the prompt and first delayed pulses, see Figure A2(a). For essentially larger values of the optical thickness ($d_p \gg 1$) the intensities of the delayed pulses are distributed such that delay time of the pulse with maximum amplitude increases, see figure A2(c) and (d). This simply follows from the dependence of the intensities of the delayed pulses, $I_k = a_k^2 \exp(-d_p/F_S) I_0$, on the optical thickness d_p, shown in figure A3 for $F = 5$ and $k = 1$, 2, and 3.

Exact solution for the harmonic AFC (see reference [17]),

$$E_{\text{out}}(t) = e^{-d_p/4} \sum_{k=0}^{+\infty} \frac{(d_p/4)^k}{k!} E_{\text{in}}(t - kT), \qquad \text{(A20)}$$

whose finesse is $F_H = 2$, shows quite different results for the large optical thickness. The line, which links maximum amplitudes of the pulses, forms a bell-shaped envelope, *i.e.* the energy of the field is smoothly distributed among the delayed pulses. Numerical analysis shows that similar results are obtained also for the square AFC for $F_S = 2$ and large d_p. However, after a series of pulses with noticeable amplitudes forming a set with a bell-shaped envelope, a series of pulse groups with much smaller amplitudes is formed. This analysis is performed by the numerical calculation of the coefficients $a_k \exp(-d_p/2F_S)$ with the help of equation

$$a_k e^{-d_p/2F_S} = \frac{1}{2\nu_0} \int_{-\nu_0}^{\nu_0} e^{-\alpha_c(\nu) l - ik\pi\nu/\nu_0} d\nu. \qquad \text{(A21)}$$

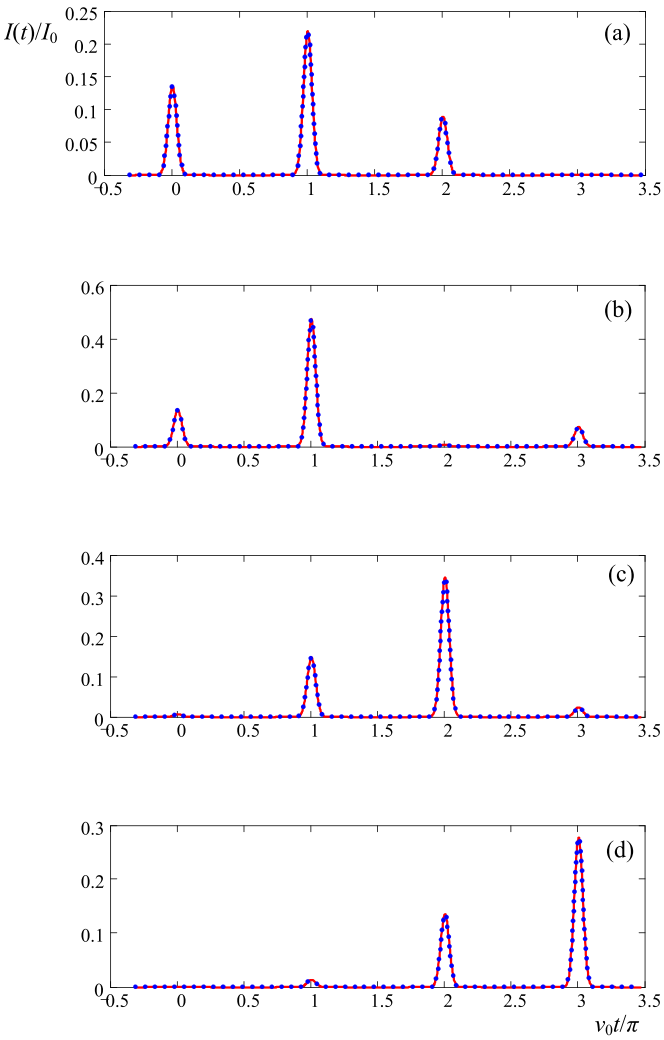

Figure A2. Time dependencies of the intensities of the pulses produced at the exit of the AFC medium whose parameters are $F_S = 2$, $d_p = 4$ (a), $F_S = 5$, $d_p = 10$ (b), $F_S = 5$, $d_p = 25$ (c), and $F_S = 5$, $d_p = 42$ (c). The values of the peak absorption parameters d_p are taken equal to those corresponding to the global maximum of the first delayed pulse in (a) and (b), the second delayed pulse (c), the third delayed pulse (d), see figure A3 as the reference for the relevant values of d_p. Solid red lines are the plots of the analytical solution equation (A19). Dotted blue lines are the numerical calculations of the inverse Fourier transformation of the solution (A9) for the Gaussian pulse $E_{\text{in}}(t) = E_0 e^{-\sigma^2 t^2}$ with $\sigma = 5\nu_0$. The number of the absorption peaks in the square AFC is 20 and the frequency integration interval is $(-4\sigma, +4\sigma)$.

Appendix B.

In this appendix the transformation of two closely spaced pulses through the square AFC comb is considered. The incident radiation consists of two Gaussian pulses

$$E_{in}(t) = E_{01} e^{-\sigma^2 (t+\tau/2)^2} + E_{02} e^{-\sigma^2 (t-\tau/2)^2 + i\varphi}, \qquad \text{(B22)}$$

where E_{01} and E_{02} are the amplitudes, φ is the relative phase, and τ is the time interval between pulses. Below, these pulses will be denoted as $E_{01}(t + \tau/2)$ and $E_{02}(t - \tau/2)$, respectively.

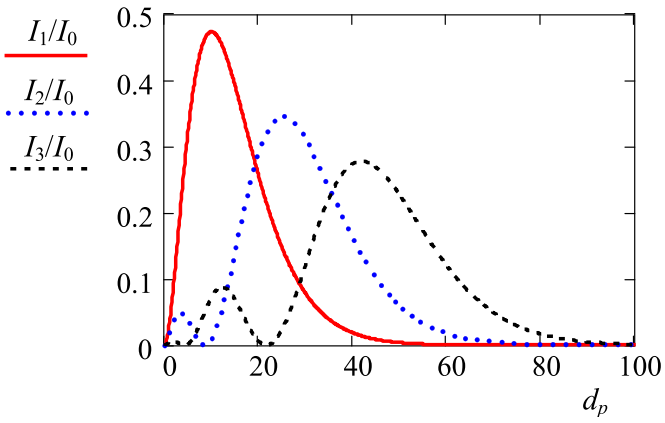

Figure A3. Dependencies of the intensities of the first I_1 (solid red line), second I_2 (dotted blue line), and third I_3 (dashed black line) delayed pulses with time delays T, $2T$, and $3T$, respectively, on the optical thickness d_p. Finesse of the square AFC is $F_S = 5$.

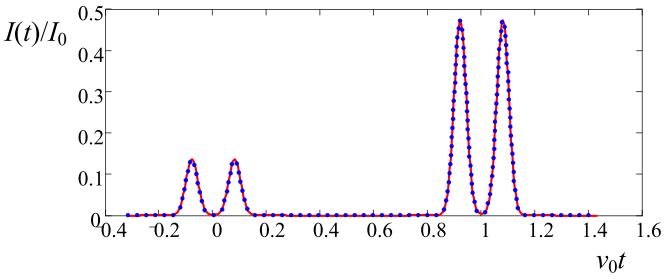

Figure A4. Time dependencies of the intensities of the couple of pulses filtered through the square AFC comb. The parameters are $F_S = 5$, $d_p = 10$, and $\sigma = 7\nu_0$. Analytical solution, equations (B23) and (B24), is shown by solid red line. Blue dotted line is the numerical calculation of the inverse Fourier transformation of the solution (A9). Frequency integration interval is $(-4\sigma,+4\sigma)$.

Since the pulses are weak and do not overlap, in the linear response approximation one can consider them separately. All second order effects such as cross-talk of the pulses are neglected.

We consider the square AFC with optimal value of optical thickness, which is $d_p = 2F_S$. Then, substantial part of the radiation field, filtered through the AFC, is concentrated in the prompt, $E_p(t)$, and delayed, $E_d(t)$, pulses. They are described as follows

$$E_p(t) = e^{-d_p/2F_S}\left[E_{01}(t+\tau/2) + E_{02}(t-\tau/2)\right], \qquad \text{(B23)}$$

$$E_d(t) = a_1 e^{-d_p/2F_S}\left[E_{01}(t-T+\tau/2) + E_{02}(t-T-\tau/2)\right]. \qquad \text{(B24)}$$

Thus, the delayed pulses have the same relation of the amplitudes and phases as the couple of the incident pulses. This case is demonstrated in figure A4.

References

[1] Ruggiero J, Le Gouët J L, Simon C and Chanelière T 2009 *Phys. Rev.* A **79** 053851
[2] Sangouard N, Simon C, Minář J, Afzelius M, Chanelière T, Gisin N, Le Gouët J L, de Riedmatten H and Tittel W 2010 *Phys. Rev.* A **81** 062333
[3] Moiseev S A and Kröll S 2001 *Phys. Rev. Lett.* **87** 173601
[4] Alexander A L, Longdell J J, Sellars M J and Manson N B 2006 *Phys. Rev. Lett.* **96** 043602
[5] Alexander A L, Longdell J J, Sellars M J and Manson N B 2007 *J. Lumin.* **127** 94
[6] Fleischhauer M and Lukin M D 2000 *Phys. Rev. Lett.* **84** 5094
[7] Phillips D F, Fleischhauer A, Mair A, Walsworth R L and Lukin M D 2001 *Phys. Rev. Lett.* **86** 783
[8] Nunn J, Walmsley I A, Raymer M G, Surmacz K, Waldermann F C, Wang Z and Jaksch D 2007 *Phys. Rev.* A **75** 011401(R)
[9] Reim K F, Nunn J, Lorenz V O, Sussman B J, Lee K C, Langford N K, Jaksch D and Walmsley I A 2010 *Nat. Photon.* **4** 218
[10] Reim K F, Michelberger P, Lee K C, Nunn J, Langford N K and Walmsley I A 2011 *Phys. Rev. Lett.* **107** 053603
[11] de Riedmatten H, Afzelius M, Staudt M U, Simon C and Gisin N 2008 *Nature* **456** 773
[12] Afzelius M, Simon C, de Riedmatten H and Gisin N 2009 *Phys. Rev.* A **79** 052329
[13] Bonarota M, Ruggiero J, Le Gouët J-L and Chanelière T 2010 *Phys. Rev.* A **81** 033803
[14] Chanelière T, Ruggiero J, Bonarota M, Afzelius M and Le Gouët J-L 2010 *New J. Phys.* **12** 023025
[15] Bonarota M, Le Gouët J-L, Moiseev S A and Chanelière T 2012 *J. Phys. B: At. Mol. Opt. Phys.* **45** 124002
[16] Sõnajalg H and Saari P 199 *J. Opt. Soc. Am* B **11** 372
[17] Shakhmuratov R N 2018 *Phys. Rev.* A **98** 043851
[18] Rippe L, Nilsson M, Kröll S, Klieber R and Suter D 2005 *Phys. Rev.* A **71** 062328
[19] Afzelius M *et al* 2010 *Phys. Rev. Lett.* **104** 040503
[20] Sabooni M, Beaudoin F, Walther A, Lin N, Amari A, Huang M and Kröll S 2010 *Phys. Rev. Lett.* **105** 060501
[21] Tschanz M, Rebane A, Reiss D and Wild U P 1996 Mol *Cryst. Liq. Crust.* **283** 43
[22] Shakhmuratov R N, Rebane A, Megret P and Odeurs J 2005 *Phys. Rev.* A **71** 053811
[23] Brendel J, Gisin N, Tittel W and Zbinden H 1999 *Phys. Rev.Lett.* **82** 2594
[24] Gisin N, Ribordy G, Tittel W and Zbinden H 2002 *Rev. Mod.Phys.* **74** 145
[25] Usmani I, Afzelius M, de Riedmatten H and Gisin N 2010 *Nat. Commun.* **1** 1
[26] Moiseev S A, Gubaidullin F F, Kirillov R S, Latypov R R, Perminov N S, Petrovin K V and Sherstyukov O N 2017 *Phys. Rev.* A **95** 012338
[27] Moiseev S A, Gerasimov K I, Latypov R R, Perminov N S, Petrovin K V and Sherstyukov O N 2018 *Sci. Rep.* **8** 3982
[28] Reshef O, Saad-Bin-Alam Md, Huttunen M J, Carlow G, Sullivan B T, Ménard J-M, Dolgaleva K and Boyd R W 2019 *Nano Lett.* **19** 6429
[29] Zhou J, Liu Z, Liu X, Pan P, Zhan X and Liu Z 2020 *Nanotechnology* **31** 375201
[30] Crisp M D 1970 *Phys. Rev.* A **1** 1604